ELUCIDATING THE IMPACT OF OXYGEN ON THE KINETIC ASSESMENT OF THE OXIDATIVE DEHYDROGENATION OF ETHANE ON A NiSnO CATALYST

Carlos Alvarado-Camacho,[a,b] Jeroen Poissonnier, [b] Joris W. Thybaut,[b] and Carlos O. Castillo-Araiza[a*]

[a] *Laboratory of Catalytic Reactor Engineering applied to Chemical and Biological Systems (LCRE)/ Ingeniería de procesos e hidráulica/Universidad Autónoma Metropolitana (UAM-I), CDMX, México.*

[b] *Laboratory for Chemical Technology, Ghent University, Technologie park 125, B-9052 Ghent, Belgium.*

**E-mail: coca@xanum.uam.mx*

Abstract

This contribution aims at evaluating the impact of oxygen conversion on the kinetic assessment of the oxidative dehydrogenation of ethane (ODH-C_2) to ethylene over a promising Ni-Sn-O catalyst in a laboratory-scale microreaction unit. On the one hand, experiments under kinetic regime were carried out in the laboratory-scale reactor. Two sets of experiments were designed to evaluate the effect of oxygen conversion on kinetics, one dataset involving 51 experiments at non-total oxygen conversion and a second dataset accounting for 60 observations at total oxygen conversion. The experiments evaluated the effect of operating condition on the catalytic performance of the reaction accounting for a mixture of ethane, oxygen and nitrogen as feedstock, at temperatures from 400 to 480ºC, inlet oxygen concentration from 1.8 to 9 % mol, space–times from 10 to 165 gcat s mol_{C2H6o}^{-1} and total pressures from 1 to 5 bar. As a response of the first set of experiments, oxygen conversion varied from 10 to 100 % whereas, in both set of experiments, ethylene selectivity varied from 45% to 90%, for an ethane conversion range from 5 to 60%. On the other hand, three mechanistic kinetic models following the steady state approach, based on Langmuir Hinshelwood Hougen & Watson (LHHW-ST), Eley Rideal(ER-ST) and Mars van Krevelen (MvK-ST) formalisms were developed to elucidate the impact of oxygen on kinetics. The development of these models used separately the two sets of experiments to elucidate their impact when characterizing kinetics in selective oxidations. Experimental results at total oxygen conversion led to apparent results in terms of selectivity to ethylene and conversion to ethane, showing in some scenarios contradictory results to those obtained at not total oxygen conversion. Nevertheless, modeling elucidated that both operating conditions led to similar selectivity and conversion trends but different kinetics parameters, which for both scenarios present phenomenological and statistical consistency. The models with the best performances were the ER and the MvK model according to the BIC criteria, suggesting that the adsorption of ethane, ethylene and CO_2 are weak adsorptions.

Keywords: *Oxidative dehydrogenation of ethane, oxygen conversion, LHHW, ER, MvK*

The authors involved in this paper are interested in submitting it to the special volume dedicated to CICAT 2020 in the international magazine Catalysis Today.

1. Introduction

The olefin market is the main building block of the chemical industry, since it covers near of 60% of the produced petrochemicals in the world [1]. The production of olefins comprising the production of ethylene and propylene is expected to continue its growing trend with an increase of approximately 19% in current capacity by 2022 [1]. Ethylene, involving around of 61% of the total olefin production, is mainly produced by steam cracking; however, this process presents several drawbacks from the economic but essentially energetic and environmental point of view; for instance: this process leads to both a high energy demand (around 17 to 21 GJ per ton of ethylene produced) and a high COx production (around 1.0 to 1.2 tons per ton of ethylene produced) [2]. In fact, although economically attractive, steam cracking is nowadays recognized as a process contributing to the global warming. Based on it, industry and academy have focused their research to propose alternative processes to produce ethylene, being the oxidative dehydrogenation of ethane (ODH-C_2) one of the most promising alternatives. Benefits of the ODH-C_2 when compared with steam cracking: I. Using a suitable catalyst the reaction temperatures are below than 500 °C (leading to a minimization of energy consumption); II. The production of CO_x is lower than in the steam

cracking process[3]; and III. availability of a cheap raw material (shale gas revolution decreased feedstock prices). Although the ODH-C_2 seems to be a convenient solution for the production of ethylene, today there is no technology at the industrial level to carry out this reaction, being one of the the main challenges for its scaling-up the design of an active, selective and stable catalyst.

Nickel oxide based catalysts are some of the most promising materials to carry out the ODH-C_2 due to their high selectivity to ethylene (higher than 80%) [4]. Specifically, a material composed of nickel oxide and tin oxide (NiSnO) has presented adequate catalytic performance, having a relatively easy and cheap method of synthesis, compared with other promising materials as the multimetallic based catalysts (MoVNbTeO). Nevertheless, there is nowadays a lack of kinetic studies evaluating the impact of operating condition on reaction rates in general and on selectivity and conversion in particular, which seems to be essential to intensify the design of the catalytic material but also establish the design bases of the reactor technology for the ODH-C_2.

According to the literature, two different types of experiments have been carried out during the ODH-C_2 on NiO-based catalysts,. In one of them, materials were evaluated at a unique operating condition elucidating their rough catalytic performance; whereas in the other one, it was evaluated the effect of one operating condition on conversion and ethylene selectivity. In the later scenario, two trends were identified. On the one hand, several works reported an increment in the selectivity to ethylene as the temperature increased [5-9]; while other studies reported opposite results [10,11]. Today, there are no studies elucidating this type of results since most of works focus on the synthesis and characterization rather than on kinetics of Ni based catalysts.

Most of kinetic studies reported in literature have developed for vanadium based catalysts. Empirical and macroscopic models have been developed for this type of materials: power law, Eley Rideal (ER), Langmuir-Hinshelwood-Hougen-Watson (LHHW) and the Mars van Krevelen. For the NiO based catalyst, it was identified only one study [54] developing a kinetic model based on a redox mechanism (MvK). Nevertheless, for both type of materials, a limited set of experiments during the kinetic analysis or the used of the quasi-equilibrium approach during the development of the model or the phenomenological or statistical inadequacy of the determined kinetic parameters led to have yet uncertainties on the understanding of the type of selective oxidation mechanism involved during the ODH-C_2 but also have a lack of understanding of steady state observations obtained out of laboratory scale reactor when developing this type of kientics studies.

This work aims at developing a kinetic assessment of the ODH-C_2 on a NiSnO under two operational scenarios in a laboratory packed bed microreactor operated under kinetic regime . In the first one, accounting for 60 independent experiments, steady state observations were obtained at total oxygen conversions. In the second one, accounting for 60 independent experiments, these observations were obtained but under not total oxygen conversion. These datasets but specifically the effect of oxygen on the catalyst bed was elucidated by developing three kinetic models following the LHHW, ER and MvK formalisms and the pseudo-steady state approach. Models and parameters were analyzed in terms of phenomenological and statistical bases.

2. Methodology

Experimental procedures

Catalyst synthesis

The bimetallic catalyst used in this study was synthesized by the evaporation method reported elsewhere[4]. The catalyst was prepared through the evaporation at 60 °C of a stirred ethanolic solution containing nickel nitrate hexahydrate, $Ni(NO_3)_2$ $6H_2O$ (Meyer, 99.5%), oxalic acid in a Ni / Additive molar ratio = 0.65, and Tin Oxalate (II), SnC_2O_4 (Sigma-Aldrich, 98%). The recovered solids were dried overnight at 120 °C; and finally are calcined for 120 minutes in static air flow at 500 ° C. A theoretical Ni/Sn atomic ratio of 20 was used in all cases.

Catalyst testing

All the catalytic experimental tests of the ODH-C_2 were carried out in a micro-reaction unit of the brand Micromeritics PID Eng & Tech model MA12216. The micro-reaction unit contains a stainless steel tubular fixed bed reactor with an internal diameter of 9 mm and a length of 305 mm which operates in isothermal mode. The test were carried out using 50, 75, 100 and 500 mg of catalyst introduced into the reactor with quartz wool as support. In addition, samples were diluted with silicon carbide in order to disperse the energy

generated by the reaction and keep a constant volume in the catalytic bed. The reaction feedstock composed of a mixture of ethane, oxygen and nitrogen with a varying composition depending on the experiment. In order to corroborate that the experiments were done in intrinsic conditions, the evaluation of limitations to the transfer of mass and heat was carried out with the procedure and the criteria reported in the literature[11]. For the analysis of the reactor effluent, the Agilent 6890N Gas Chromatograph (GC), equipped with two detectors connected in series, a flame ionization detector (FID) and a thermal conductivity detector (TCD), and one column of the HP-PLOT Q type was used. The experiments were carried out in a wide range of operating conditions at steady-state regime, this was ensured by performing 5 analyses at different times with 5% maximum deviation. A carbon balance, % C, was made to evaluate the quality of the experiment obtaining carbon balances between 95-105%. The ethane conversion Eq. (1) is calculated from its inlet F_{C2H60} and outlet F_{C2H6} molar flow rates as follows:

$$X_A = \frac{F_{C_2H_6,0} - F_{C_2H_6}}{F_{C_2H_6,0}} \times 100 \quad (2)$$

The selectivity to a n product referred to as S_n (Eq. (2)) were based on a carbon mass balance and calculated as follows:

$$S_n = \frac{F_n C_n}{2\left(F_{C_2H_6,0} - F_{C_2H_6}\right)} \times 100 \quad (3)$$

where C_n is the product carbon number and F_n is the outlet flow rates of the product n. The value of 2 represents the reactant's carbon number.

Kinetic modelling

Based on the experimental observations the global reaction network employed for the kinetic modeling of the ODH-C_2 involves all species observed in the gas chromatograph analysis. The scheme includes reactions in parallel as well as consecutive reactions. Ethylene is produced from the oxidative dehydrogenation of ethane (r_1), and the carbon dioxide (CO_2) can be form from the combustion of ethane (r_2) or ethylene (r_3). Considering this reaction network, different kinetic models following the steady state approach were developed to elucidate the effect of oxygen on kinetics in the studied laboratory reactor for the ODH-C_2 on a NiSnO material. Models are based on different mechanistic formalisms, including LHHW, ER and MvK. For sake of brevity, LHHW is the only model presented din this document.

The LHHW kinetic model was developed considering the following main assumptions: I. catalyst consists of one type of active sites (*); II. There is a competitive adsorption of reactants (ethane and oxygen) and products (ethylene, carbon oxides and water) for the active sites; III. Based on thermodynamics, surface reactions are irreversible; IV. The adsorption of oxygen is dissociative; and V. All products are susceptible to be re-adsorbed on the active sites. Table 1 includes the reaction steps that are taken into account for the construction of the kinetic model (where * represents the active sites). In Table 1, σ_j represents the stoichiometric number of Horiuti used to describe the number of times that the adsorption, reaction and desorption steps must occur, to complete a catalytic reaction cycle according to the general reaction network scheme, represented by steps I to III.

Table 1 Reaction steps and catalytic cycles considered for the LHHW model.

	Reaction step	σ_I	σ_{II}	σ_{III}
A	$O_{2(g)} + 2* \rightleftharpoons 2\,O*$	1	7	3
B	$C_2H_{6(g)} + * \rightleftharpoons C_2H_6*$	2	2	0
1	$C_2H_6* + O* \longrightarrow C_2H_4* + H_2O*$	2	0	0
2	$C_2H_6* + O* \rightsquigarrow \ldots \xrightarrow{+6O*} 2\,CO_2* + 3\,H_2O* + 3*$	0	2	0
3	$C_2H_4* + O* \rightsquigarrow \ldots \xrightarrow{+5O*} 2\,CO_2* + 2\,H_2O* + 3*$	0	0	1
C	$C_2H_4* \rightleftharpoons C_2H_{4(g)} + *$	2	0	1
D	$CO_2* \rightleftharpoons CO_{2(g)} + *$	0	4	2
E	$H_2O* \rightleftharpoons H_2O_{(g)} + *$	2	6	2
I	$C_2H_6 + 0.5\,O_2 \longrightarrow C_2H_4 + H_2O$			
II	$C_2H_6 + 3.5\,O_2 \longrightarrow 2\,CO_2 + 2\,H_2O$			
III	$C_2H_4 + 3.0\,O_2 \longrightarrow 2\,CO_2 + 2\,H_2O$			

The proposed mechanism involves 8 kinetic steps taking place on the catalyst surface. The reaction rate of the surface steps can be expressed according with the law of mass action:

$$r_j = \vec{k}_j \prod \left[i^*\right]^{\nu_{i,j}} \quad (3)$$

Oxygen adsorption/desorption:

$$r_{A^f} = k_A^f p_{O_2} N_T \theta_S^2 \quad , \quad r_{A^b} = k_A^b N_T \theta_O^2 \quad (4)$$

Ethane adsorption:

$$r_{B^f} = k_B^f p_{C_2H_6} N_T \theta_S \quad , \quad r_{B^b} = k_B^b N_T \theta_{C_2H_6} \quad (5)$$

Reaction 1: $r_1 = k_1 N_T \theta_{C_2H_6} \theta_O$ (6)

Reaction 2: $r_2 = k_2 N_T \theta_{C_2H_6} \theta_O$ (7)

Reaction 3: $r_3 = k_3 N_T \theta_{C_2H_4} \theta_O$ (8)

Ethylene adsorption/desorption:

$$r_{C^f} = k_C^f N_T \theta_{C_2H_4} \quad , \quad r_{C^b} = k_C^b p_{C_2H_4} N_T \theta_S \tag{9}$$

CO_2 adsorption/desorption:

$$r_{D^f} = k_D^f N_T \theta_{CO_2} \quad , \quad r_{D^b} = k_D^b p_{CO_2} N_T \theta_S \tag{10}$$

H_2O adsorption/desorption:

$$r_{E^f} = k_E^f N_T \theta_{H_2O} \quad , \quad r_{E^b} = k_E^b p_{H_2O} N_T \theta_S \tag{11}$$

Considering isothermal operation and negligible pressure drop over the reactor, the 1-D pseudo-homogeneous model for plug flow can be employed, see Eq.

$$\frac{dF_i}{dW} = R_i \quad i = 1 \ldots n_{resp} \tag{12}$$

with $F_i = F_{i,o}$ at $W = 0$ (13)

as initial conditions. In the above equations, W represents the catalyst mass, F_i and $F_{i,0}$ the molar outlet and inlet flowrate of the i component respectively, R_i the net production rate of component, n_{resp} number of responses.

The net formation rate R for every response is defined as the sum of rates of the reactions it is involved into taking into account the formation or consumption coefficient:

$$R_i = \sum_i \upsilon_{ij} r_j \tag{11}$$

where υ_{ij} is a stoichiometric coefficient of component *i* in reaction *j*.

According to the proposed models, several kinetic coefficients arised: reverse and forward adsorption coefficients (k_{if} and k_{ib}), adsorption equilibrium coefficients (K_i), and reaction coefficients (k_j).

The temperature dependence of the rate coefficients was expressed by the Arrhenius equation. The values for pre-exponential factors were calculated a-priori based on statistical thermodynamics and kept fixed during further regression. It made used of the the transition state theory, where the the entropy change between the reactant and transition state ($\Delta S_j^{0,\neq}$) was determined but accounting for assumptions on the loss of or gain in degrees of freedom Entropies of surface species and transition states were calculated from entropies of the associated molecules in the gas phase and the standard entropy change corresponding to the chemisorption step. For instance, r the entropy change due to the chemisorption was quantified considering an specific loss of translational degrees of freedom, approximating its value by using the Sackur-Tetrode equation. This consideration is formally valid for transition state species pre-exponential factors for the backward steps, but obtained using the principle of microscopic reversibility, where standard entropies of the associated molecules of the chemisorbed species in gas phase were obtained directly from empirical sources.

Parameter estimation

Energies involved in the kinetic models were estimated by minimizing a weighted objective function referred to as *RSS(ß)*, which includes the residual sum of squares of the molar flow rates of all the species accounted.

$$RSS(b) = \sum_{i=1}^{n_{resp}} \sum_{j=1}^{n_{exp}} w_i \left(F_{i,j} - \hat{F}_{i,j} \right)^2 \xrightarrow{b_1, b_2, \ldots b_n} min \tag{36}$$

where β is the optimal parameters vector, n_{exp} is the number of independent experiments, n_{resp} is the number of responses, $F_{i,j}$ and and $\hat{F}_{i,j}$ are the i-th experimental and predicted responses for the j-th observation, respectively, and w_i is the weight factor assigned to the i-th response.

When calculating the objective function in Eq. (36), depending the case (experiments at not-total or at total oxygen conversion), the summation was performed over 51 or 60 observations, each including five responses, i.e., the molar outlet flow rates of ethane, ethylene, CO_2, oxygen and water.

The weighting factor w_i was calculated for each response and corresponds to the diagonal elements of the inverse of the variance-covariance matrix of the experimental erro

3. Results and discussion

Experimental results

The experimental dataset for the ODH-C_2 on NiSnO was collected with the focus on variation of operating conditions and includes 111 experiments to intrinsic kinetic data acquisition, 51 experiments at no-total oxygen conversion and 60 at full oxygen conversion.

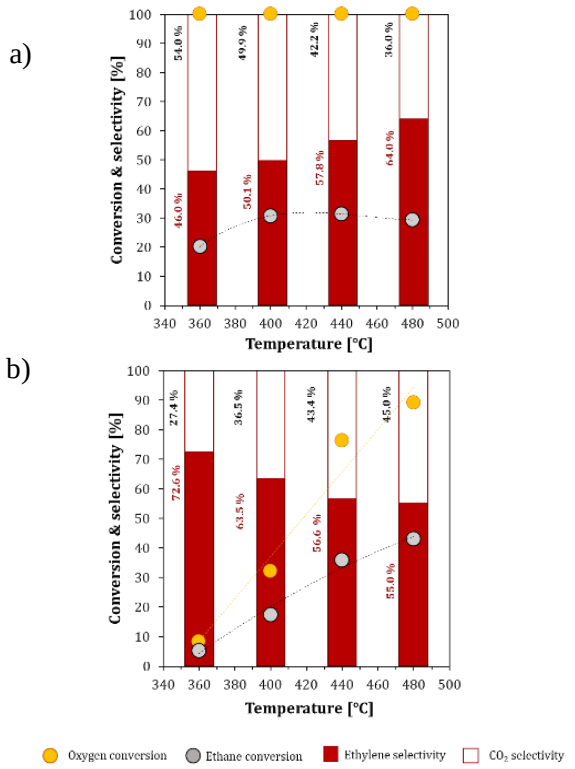

Figure 2. Ethane and oxygen conversion, and CO_2 and ethylene selectivity as a function of temperature a) total O_2 conversion and b) non-total O_2 conversion.

One of the most important variables affecting the performance of the ODH-C_2 is the temperature. As also reported in literature for other Ni based materials, two different trends were identified for NiSnO catalysts. For total oxygen conversion, Figure 2a, ethylene selectivity increases with the temperature from 46% at 350 °C to 64% at 480 °C and ethane conversion is maintained constant after 400 °C. An unexpected results for selective oxidations where increments in temperature favor the production of CO_2. On the other hand, Figure 2b, at no total oxygen conversions, the conversion of ethane and oxygen increased as the temperature increased as well, from 5 to 43 % and from 8 to 90 %, respectively. However, in the later, it is worth observing that that temperature favors total oxidation of hydrocarbons, resulting in an increase in ethane conversion but a decrease in the selectivity to ethylene. Similar results were obaied when evaluating the effect of the space time and the inlet oxygen concentration.

Parameter values were obtained by the weighted regression for the ST-LHHW model, using the data set of non-total oxygen conversion and the one at full oxygen conversion. For sake of brevity, this document only present a results obtained by LHHW model. All parameters estimated were statistically significant with very narrow confidence intervals with phenomenological sounds. In terms of the regression, F value for the global significance for table 4 was 1145 and for table 5 was 321, such values significantly exceed the tabulated value for both cases. In addition the highest binary coefficients were 0.88 and 0.7, respectively. In Figure x, the parity diagram of the five responses is shown for the two sets. This type of diagrams are commonly used to represent the capability of the models of adequately describing the experimental observations.

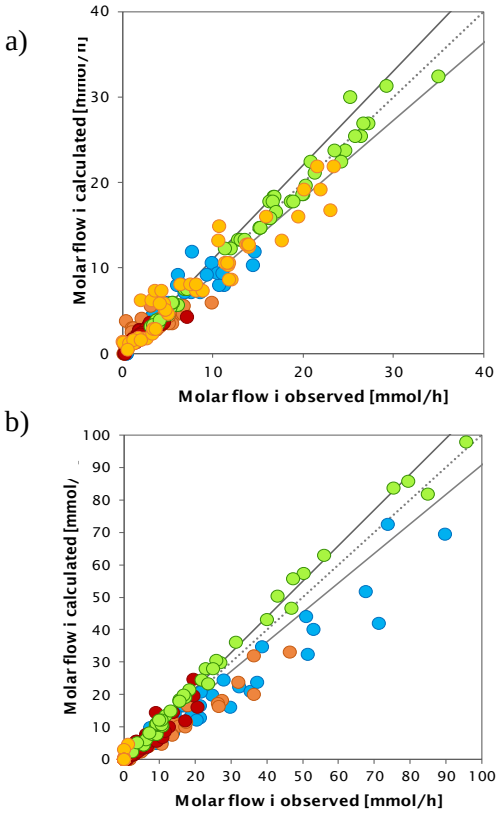

Figure X. Parity plots comparing experimental with calculated reactor outlet molar flow rates. a)Non-total oxygen conversion, and b) Total oxygen conversion.

Related to the phenomelogical meaning of the parameters, the activation energies were very similar in both studied cases, increasing according to the following order: $Ea_{,1} < Ea_{,2} < Ea_{,3}$. The lowest reaction activation energy was obtained for the selective oxidation of ethane, which makes sense since the total oxidation requires higher activation energies to take place. In addition, according with the literature, activation energies higher than 210 kJ/mol indicate catalyst deactivation by sintering. In

this respect, any estimated value of activation energy exceeds this limit[13].

Related to the adsorption parameters, they accomplished the Boudart criteria[14]. However, in this case the adsorption enthalpies, they change greatly depending on the set used. Figure Xa and Xb display the distribution of adsorbed species on the catalyst surface. Their performance is totally different. For the non-total oxygen conversion set, the predominant specie on the catalyst surface was the oxygen, while for the total oxygen conversion set it was the water, stressing the importance of an adequate analysis of experiments to characterize kinetics of a catalytic reaction..

a)

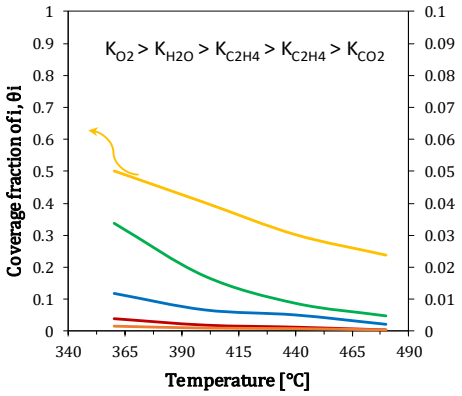

b)

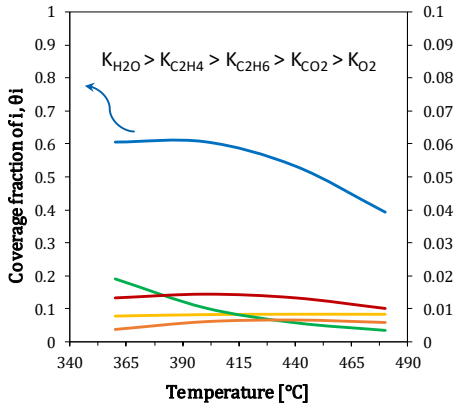

Figure X. Simulations varying the temperature, distribution of the adsorbed species on the catalyst surface for the a)Non-total oxygen conversion, and b) Total oxygen conversion.

Conclusions

A kinetic study of the ODH-C_2 was undertaken over a promising NiSnO catalyst, using experimental sets at non-total and total oxygen conversion under kinetic regime. Experimental results, demonstrated that oxygen conversions leads to different trends on the ethane conversion and selectivity to ethylene. Modelling allows the elucidation of kinetics at both studied experimental conditions, however, observations led to obtain different performance of the oxygen on the catalyst surface, which is widely discussed in the extended version of the manuscript.

4. Acknowledgment

CONACyT and UAM-I for the financial support for carrying out this research.

5. References

[1] OPEC, World Oil Outlook 2040. 2017.

[2] Ren, T., Patel, M. and Blok, K. Energy 31, 425–451, 2006.

[3] Gärtner A., et al., ChemCatChem. 5(11): p. 3196-3217, 2013.

[4] Solsona, B., et al., Journal of catalysis. 295: p. 104-114, 2012.

[5] Ducarme V. and Martin G.A. Catalysis Letters 23, 97-101, 1994

[6] Lin X., et al., Journal of Catalysis 265, 54–62, 2009.

[7] Lin X. et al. Applied Catalysis A: General 381, 114–120, 2010.

[8] Ykrelef A. et al. Catalysis Today 299, 93–101, 2018.

[9] Nakamura K. et al. Journal of Molecular Catalysis A: Chemical, 144–151, 2006.

[10] Ştefan-Bogdan I. et al. Catal. Sci. Technol., 6, 6, 953, 2016.

[11] Zhu H.,et al. J. Catal. 285, 292–303, 2012.

[12] Thybaut J. W. Encyclopedia of Catalysis, Book chapter, 2010.

[13] Santacesaria E. Catal. Today 34, 393–400, 1997.

[14] Boudart M., Mears D.E., Vannice M.A. Ind. Chim. Belg. 32, 281–284, 1967.